**Proceedings of the 2016 11th International Pipeline Conference**
**IPC2016**
**September 26-30, 2016, Calgary, Alberta, Canada**

**IPC2016-64050**

# A NEW APPROACH TO DETERMINE THE STRESSES IN BURIED PIPES UNDER SURFACE LOADING

**Fan Zhang, PhD**
Kiefner and Associates Inc.
Columbus, OH, USA

**Nathan Branam**
Kiefner and Associates Inc.
Columbus, OH, USA

**Benjamin Zand, PhD**
Kiefner and Associates Inc.
Columbus, OH, USA

**Mark Van Auker**
Kiefner and Associates Inc.
Columbus, OH, USA

## ABSTRACT

All buried pipes experience loading from the weight of soil overburden. When pipelines cross railroads, roads, parking lots or construction sites, the pipes also experience live surface loading from vehicles on the ground, including heavy construction equipment in some scenarios. The surface loading results in through-wall bending in pipes, which generates both hoop stress and longitudinal stress. Current standards limit the stresses in buried pipes to maximum values in terms of hoop stress, longitudinal stress and combined biaxial stress. An early approach to estimating stresses and deformations in a pipe subjected to surface loads dates back to Spangler's work in the 1940s. Many models have been developed since then. API RP 1102 provides guidance for the design of pipeline crossings of railroads and highways following the model developed by Cornell University for the Gas Research Institute (GRI). The Cornell model was developed only based on experiments on bored pipes crossing a railroad or a highway at a near-right angle. The live surface loading distribution is also limited to the wheel-layout typical of railroad cars and highway vehicles. Most other existing models only focus on the hoop stress in the pipe. In this paper, a new approach to determine the stresses in buried pipes under surface loading is introduced. The approach is suitable for assessing pipes beneath any type of vehicle or equipment at any relative position and at any angle to the pipe. First, the pressure on the pipe from surface loading is determined through the Boussinesq theory. Second, both hoop stress and longitudinal stress in the pipe are estimated. The hoop stress is estimated through the modified Spangler stress formula proposed by Warman and his co-workers (2006 and 2009). The longitudinal stress, due to local bending and global bending, is estimated by the theory of beam-on-elastic-foundation. The modulus of foundation can be determined through the soil-spring model developed by ASCE. The hoop stress, longitudinal stress and the resulting combined biaxial stress can then be compared against their respective limits from a pertinent standard to assess the integrity of the pipe and determine the proper remediation approach, if necessary. The performance of the proposed approach is compared in this study with the experimental results in the literature and the predictions from API RP 1102.

## INTRODUCTION

The pipeline industry has had a vested interest in stresses in buried pipes due to surface loading since Spangler, at Iowa State University, conducted the pioneer work on the topic in the 1940s [1,2,3,4]. Spangler computed hoop stresses in buried pipe with the consideration of the stiffness effect from internal pressure. The formula was known as the "Spangler stress formula", and was later used in an early version of API RP 1102 [5]. He also developed an equation to compute ovality in buried culverts, known as the "Iowa formula", which accounts for bearing support from soil surrounding the pipes.

A multi-year project, sponsored by GRI and conducted by researchers at Cornell University [6,7,8], developed formulae based on finite element analysis (FEA) of bored installed pipes under surface loads. The formulae estimate both hoop stress and longitudinal stress resulting from surface loads, which enable a more accurate estimation of combined biaxial stress. The combined biaxial stress is a more suitable measure of yielding risk than hoop stress alone. Further experiments involving two bored pipes under railroad loads helped to verify the performance of this method. These formulae were later adapted in the current version of API RP 1102 [9]. It is worth noting that the formulae do not consider the changes of stiffness from internal pressure variation, and the application range is limited by the range of pipe dimensions and buried depths investigated by FEA.

Warman et al. [10,11] proposed a modified Spangler stress formula, which is also known as "CEPA equation". The CEPA equation combines the advantages of the original "Spangler stress formula" and the "Iowa formula", which enables it to consider the influence of both internal pressure and the support of the surrounding soil to the predicted hoop stress. Francini and Gertler later found the amplitude of longitudinal stress can be as high as or higher than the hoop stress from their tests [12], which motivated Van Auker and Francini to add the prediction of longitudinal stress in their CEPA surface loading calculator [13].

API RP 1102 is one the most widely used approaches to estimate the stress in buried pipe under surface loading. However, practical application of this approach creates frequent engineering challenges due to its limitations. Some of the limitations include the limited range of buried pipe depths for which it can be applied, the limited range of diameter to wall thickness ($D/t$) ratios for which the approach is applicable, and the need for the crossing angle between the pipe and the road to be near 90°. Since the method was developed based on FEA for bored pipes, the application of this approach on pipes installed using the open trench method becomes questionable.

In this paper, a new approach to estimate the stress in buried pipes resulting from surface loads is presented. This approach is based on Van Auker and Francini's work [13] with revisions in the method of estimating longitudinal stress. In the first section, the detailed approach is introduced. In the second section, the performance of the new approach is verified by comparison with collected experimental data. The prediction is also compared with that from the current API RP 1102 approach. Discussions regarding the new approach are presented in the third section, and conclusions are summarized at the end of the paper.

## APPROACH TO DETERMINE THE STRESSES IN BURIED PIPES UNDER SURFACE LOADING

Surface loading on buried pipes originates from two sources: the live load on the ground surface and the soil overburden on top of the pipe.

### Stress from Live Load

The pressure at the pipe surface from live surface loads on the ground can be calculated by the Boussinesq equation as

$$p_{\mathrm{live}} = \frac{3P_{\mathrm{surf}}}{2\pi H^2\left[1+\left(\frac{z}{H}\right)^2\right]^{\frac{5}{2}}} F_{\mathrm{impact}} \tag{1}$$

where $p_{\mathrm{live}}$ is the pressure on the pipe due to the live surface load, $P_{\mathrm{surf}}$ is the concentrated load on the ground surface, $z$ is the horizontal offset of the measurement point on the pipe from the location that the concentrated load is applied on the ground, $H$ is the depth of cover (DoC), and $F_{\mathrm{impact}}$ is the impact factor to account for the dynamic impact of a moving vehicle.

The Boussinesq equation assumes a homogeneous elastic foundation and provides a conservative estimation for a road with a hard layer at the top surface. The Boussinesq equation has been accepted by the pipeline industry, is used in early versions of API RP 1102 [5], and is also used in the later developed Guidelines for the Design of Buried Steel Pipe [14]. The Boussinesq equation can be generalized to any type of surface loading by integrating contact pressure over the contact areas between wheels or tracks and the ground. Assuming the pressure in a contact area is uniform and equals the internal tire pressure in the pneumatic tire, the area can be divided into a grid of small rectangles with a concentrated load on each rectangle that equals the pressure times the area of the rectangle. The total pressure at a given underground point can then be obtained by summing the contribution from each rectangle to the pressure point. Maximum live pressure on a pipeline can be determined by varying the location of the vehicle with respect to the pipe and repeating the calculations. This maximum pressure is then used to calculate the stress in the pipe.

The original Boussinesq equation only estimates the static load. The impact factor, $F_{\mathrm{impact}}$, in equation (1) helps to account for dynamic loading from the moving vehicle. The impact factor generally ranges from 1.0 to 1.5. While there is no explicit guidance on choosing impact factor, the dynamic loading is affected by vehicle speed, tire pressure, ground unevenness and depth of cover.

The pressure from the live load results in both hoop stress and longitudinal stress in the buried pipe. The CEPA equation [10,11] can be used to determine the hoop stress from the live load as

$$\sigma_{\mathrm{H\_live}} = \frac{3K_{\mathrm{b}} p_{\mathrm{live}}\left(\frac{D}{t}\right)^2}{1+3K_{\mathrm{z}}\frac{p_{\mathrm{i}}}{E}\left(\frac{D}{t}\right)^3+0.0915\frac{E'}{E}\left(\frac{D}{t}\right)^3} \tag{2}$$

where $K_{\mathrm{b}}$ is the bending moment parameter, $D$ and $t$ are the pipe outside diameter (OD) and wall thickness (WT) respectively, $K_{\mathrm{z}}$ is the deflection parameter, $p_{\mathrm{i}}$ is the internal pressure of the pipe, $E'$ is the modulus of soil reaction, and $E$ is the elastic modulus of steel. The parameters $K_{\mathrm{b}}$ and $K_{\mathrm{z}}$ were provided by Spangler [4] as shown in Table 1. For pipes installed using an auger boring method, a large bedding angle of 120° can be assumed. For pipes installed using an open trench method, it is conservative to use a bedding angle of 30°, as the bottom reaction occurs over an arc of 30° to 60° [15]. Table 2 lists the values for $E'$ recommended by Hartley and Duncan [16].

The longitudinal stress in the pipe resulting from a live load on the ground has two components. The first, $\sigma_{\mathrm{L\_live\_lb}}$, is due to local bending in the pipe wall under the distributed load on the pipe surface. It can be determined using Bijlaard's solutions for local loading on a pipe [17] as

 

$$\sigma_{\text{L\_live\_lb}} = \frac{0.153}{1.56}\sqrt{12(1-\nu^2)}\sigma_{\text{H\_live}} \tag{3}$$

where $\nu$ is the Poisson's ratio of steel.

**Table 1. Values of Parameters $K_b$ and $K_z$**

| Bedding Angle (deg) | Moment Parameter, $K_b$ | Deflection Parameter, $K_z$ |
|---|---|---|
| 0 | 0.294 | 0.110 |
| 30 | 0.235 | 0.108 |
| 60 | 0.189 | 0.103 |
| 90 | 0.157 | 0.096 |
| 120 | 0.138 | 0.089 |
| 150 | 0.128 | 0.085 |
| 180 | 0.125 | 0.083 |

**Table 2. Typical Values of the Modulus of Soil Reaction, $E'$ (in psi).**

| Type of Soil | DoC* (ft) | Standard AASHTO# Relative Compaction | | | |
|---|---|---|---|---|---|
| | | 85% | 90% | 95% | 100% |
| Fine-grained soils with less than 25% sand content (CL, ML, CL-ML) | 0-5 | 500 | 700 | 1,000 | 1,500 |
| | 5-10 | 600 | 1,000 | 1,400 | 2,000 |
| | 10-15 | 700 | 1,200 | 1,600 | 2,300 |
| | 15-20 | 800 | 1,300 | 1,800 | 2,600 |
| Coarse-grained soils with fines (SM, SC) | 0-5 | 600 | 1,000 | 1,200 | 1,900 |
| | 5-10 | 900 | 1,400 | 1,800 | 2,700 |
| | 10-15 | 1,000 | 1,500 | 2,100 | 3,200 |
| | 15-20 | 1,100 | 1,600 | 2,400 | 3,700 |
| Coarse-grained soils with little or no fines (SP, SW, GP, GW) | 0-5 | 700 | 1,000 | 1,600 | 2,500 |
| | 5-10 | 1,000 | 1,500 | 2,200 | 3,300 |
| | 10-15 | 1,050 | 1,600 | 2,400 | 3,600 |
| | 15-20 | 1,100 | 1,700 | 2,500 | 3,800 |

* DoC: Depth of cover

# AASHTO: the American Association of State Highway Transportation Officials

The second component, $\sigma_{\text{L\_live\_gb}}$, is due to the global bending of the pipe segment under the live load as

$$\sigma_{\text{L\_live\_gb}} = \frac{MD}{2I} \tag{4}$$

where $M$ is the bending moment and $I$ is the moment of inertia of the pipe cross section calculated as

$$I = \frac{\pi}{4}\left[\left(\frac{D}{2}\right)^4 - \left(\frac{D}{2} - t\right)^4\right] \tag{5}$$

The bending moment $M$ can be determined by the solution of beam on elastic foundation [18] considering that the pipe experiences a uniform distributed load, $W_i$, on a segment with a length of $l_i$ as shown in Figure 1. The distance from a measurement point on the pipe to the two ends of the segment with the distributed load is $a_i$ and $b_i$, respectively. The bending moment, $M_i$, at the measurement point on the pipe due to load $W_i$ is

$$M_i = \frac{W_i}{4\lambda^2}F(a_i, b_i) \tag{6}$$

If the measurement point is inside the segment with the distributed load as shown in Figure 1 (a), the $F(a_i, b_i)$ is

$$F(a_i, b_i) = e^{-\lambda a_i}\sin(\lambda a_i) + e^{-\lambda b_i}\sin(\lambda b_i) \tag{7}$$

If the measurement point is outside the segment with the distributed load as shown in Figure 1 (b), the $F(a_i, b_i)$ is

$$F(a_i, b_i) = e^{-\lambda b_i}\sin(\lambda b_i) - e^{-\lambda a_i}\sin(\lambda a_i) \tag{8}$$

In equation (8), it is assumed that $a_i > b_i$. The coefficient $\lambda$ in equations (6) to (8) is

$$\lambda = \sqrt[4]{\frac{k}{4EI}} \tag{9}$$

where $k$ is the spring coefficient of the soil providing the resistance to the deflection of the pipe. It can be determined as $k = k_0 D \sin(\Omega/2)$, where $\Omega$ is bedding angle and $k_0$, in the unit of pressure/length, is the elastic spring constant (also known as modulus of the foundation) which is based on soil type as listed in Table 3 [18].

**Table 3. Values of Modulus of the Foundation, $k_0$**

| Soil Type | Range in lb/in$^3$ | | Range in N/mm$^3$ | |
|---|---|---|---|---|
| | Min | Max | Min | Max |
| Loose Sand | 18.42 | 58.94 | 0.005 | 0.016 |
| Medium Sand | 36.84 | 294.71 | 0.010 | 0.080 |
| Dense Sand | 232.08 | 471.53 | 0.063 | 0.128 |
| Clayed Sand(Medium) | 114.20 | 294.71 | 0.031 | 0.080 |
| Silty Sand (Medium) | 88.41 | 176.82 | 0.024 | 0.048 |
| Clay, $q_u$*<0.2 N/mm$^2$ | 44.21 | 88.41 | 0.012 | 0.024 |
| Clay, 0.2<$q_u$<0.4 N/mm$^2$ | 88.41 | 176.82 | 0.024 | 0.048 |
| Clay, $q_u$ > 0.4 N/mm$^2$ | 176.82 | | 0.048 | |

* $q_u$: unconfined compressive strength

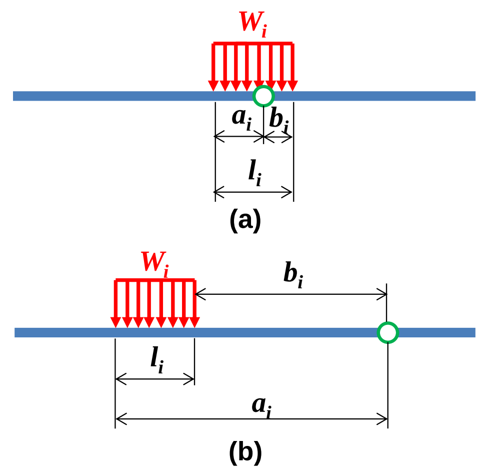


**Figure 1. Illustration of Pipe under a Distributed Load $W_i$ over a Segment with Length $l_i$.**

Alternatively, the spring coefficient, $k$, can be determined from the pipe soil interaction model as described in Annex A of the paper. Finally, the bending moment, $M$, at a specified point on the pipe, can be determined by summing up $M_i$ in equation (6) at every small segment along the pipe as

$$M = \sum_i M_i \tag{10}$$

### Stress from Soil Overburden

For pipe buried at shallow to moderate depth, the pressure at the pipe surface from soil loading is estimated by prism load of the column of soil over the pipe as

$$p_{\text{soil}} = \gamma H \tag{11}$$

where $\gamma$ is the weight of soil per unit volume. The prism load is conservative and recommended by Moser [19] for flexible pipe. The resulting hoop stress, $\sigma_{\text{H\_soil}}$, can then be determined via equation (2) by replacing $p_{\text{live}}$ with $p_{\text{soil}}$ from equation (11).

For a deep-buried pipe, the arching effect helps to distribute part of the prism load to the soil surrounding the pipe. For this scenario, using the prism load approach is overly conservative and an alternative approach, such as that in API RP 1102 [9], can be used to determine the hoop stress from the soil load.

The longitudinal stress resulting from soil overburden is uniformly distributed along a buried pipe. As the axial deformation of a buried pipe is restrained by the soil, the longitudinal stress is determined by the Poisson effect as

$$\sigma_{\text{L\_soil}} = \nu \sigma_{\text{H\_soil}} \tag{12}$$

## PERFORMANCE OF THE APPROACH

The performance of the approach introduced above was checked by comparing the predictions from the approach with experimental results collected from literature and the predictions from the current API RP 1102 approach. Only the stresses generated by live loads were investigated as a) limited tests reported the stresses from soil overburden, b) thorough studies have been conducted by other researchers [19] on stresses in buried pipes from soil overburden, and c) the stresses from live loads generally dominates the integrity discussion of pipes under surface loading.

### Collected Experimental Results

The experimental results from the work by three different groups were collected.

<u>Battelle and AARRC</u>

The experiments were conducted by the Association of American Railroads Research Center (AARRC) from 1960 to 1967. The data was later analyzed by Battelle Memorial Institute in a summary report to the Research Council on Pipeline Crossings of Railroads and Highways of American Society of Civil Engineers [20]. The report covers the experimental results on an 8.625-inch diameter, 0.219-inch wall thickness pipe and a 24-inch diameter, 0.25-inch wall thickness pipe. The pipes were installed by open trench method in silty sand soil within confining timber bulkheads. The soil was compacted to approximately 95% of its standard Proctor density after the pipe was installed, and before any experiments were conducted. The buried depth of the 8.625-inch pipe was 27.375 inches. Two buried depths of 25 inches and 50 inches were investigated on the 24-inch pipe.

Two loading configurations were used to apply live loads on the 8.625-inch pipe. A three-tie track segment, as shown in Figure 2, was used to simulate a railroad load. Each tie was 7-inches high, 9-inches wide, and 8.5-feet long. The space between the close edges of two adjacent ties was 11 inches as shown in Figure 2. The length of the ties was along the pipe axial direction. The load amplitude applied on the track segment increased from 18 kips up to 95 kips. A total of 2,000,000 cycles of 95 kips force through the three-tie track segment was then applied to simulate the ground compacting at the crossing over a long period of time. The 95 kips load was then applied again to determine the influence of the compaction. After that, the loading configuration of a 15-inch diameter steel plate was used to simulate the point load on unpaved ground. The investigated amplitudes of the load were 10 kips and 15 kips. The internal pressure was zero during the application of all live loads on the 8-inch pipe.

Three loading configurations were used to apply live loads on the 24-inch pipe. An 8-foot long, 6-foot wide and 6-inch thick concrete slab was used to simulate the load on a road with rigid pavement. The length of the slab was along the pipe axial direction. The load amplitude was 25 kips. The same steel plate in the experiments on the 8.625-inch pipe was then used to apply a 25 kips point load. Finally, the same three-tie track segment in the experiments on the 8.625-inch pipe was used to apply a 95 kips railroad load. The live loads were applied before compacting the soil with cyclic loads. All live loads were applied on the pipe with zero internal pressure and also with 550 psig internal pressure.

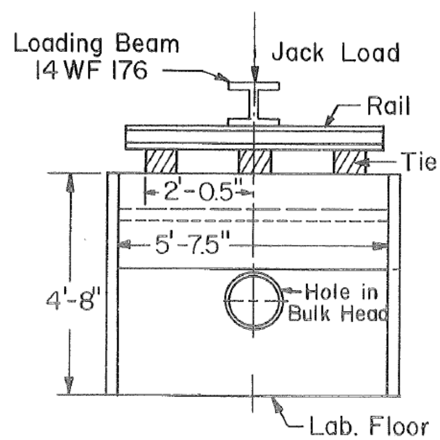


**Figure 2. Transverse Section through Simulated Crossing with Three-Tie Track Segment (Battelle and AARRC) (from Figure 2 in Reference [20])**

Spangler

The second work was a field casing investigation led by Spangler in the 1960s [21]. The test data consisted of three casing pipes installed at Thorsby, Alabama, one at Gallup, New Mexico, and one at Garden City, Iowa. The tests were conducted over multiple years. Only the maximum hoop stresses due to the passage of trains on the tracks above the pipes were recorded. As these were casing pipes, there was no internal pressure applied during the tests.

Cornell and TTC

The third work was conducted by a research group from Cornell University at the Transportation Test Center (TTC) from 1988 to 1990 [8]. These experiments were part of the effort to develop the approach in the current version of API RP 1102. A 12.75-inch diameter, 0.250-inch wall thickness, X42 pipe and a 36-inch diameter, 0.606-inch wall thickness, X60 pipe were installed using auger boring methods. The soil type at the site was reported as dense sand. The depth of cover for both pipes was 5.75 feet. In reference [8], the maximum hoop stress and longitudinal stress were measured when a train was over the pipe.

The pipe dimensions, buried depth, installation method, soil type, and internal pressure level of above collected experimental data are summarized in Table 4. The loading method and load amplitude are summarized in Table 5.

## Analysis with Kiefner Approach

To facilitate the late comparison, the approach introduced previously in the paper is referred to as the Kiefner approach. The input parameters[i] for the analysis with the Kiefner approach are listed in Table 6.

The modulus of soil reaction, $E'$, depends on soil type, buried depth of the pipe, and compaction of backfills as shown in Table 2. In the Battelle-AARRC experiments, the silty sand soil was compacted to 95% of its standard proctor density before the application of live loads. From Table 2, $E'$ is 1,200 psi based on 95% compacted coarse-grained soils with fines (SM, SC) buried deeper than 5 feet. For the 8.625-inch pipe, some of the experiment was conducted after further compacting of the soil with 2,000,000 cycles of load. No significant changes of stresses in the pipe were observed after the first 500,000 cycles of load. The soil should have been fully compacted to 100%. Therefore, a modulus of soil reaction of 1,900 psi was assumed for the experiments after the additional loading cycles were applied. In the Spangler experiments, no detailed information was available for the type of soil at the sites. Since the tests were conducted under the rail road over multiple years, it was reasonable to assume the soil had reached 100% compaction. The types of soil were deduced from the measured stress level[ii] as follows. In the Spangler experiments conducted at Thorsby, Alabama, the three casing pipes were buried at the shallowest depth of 7 feet but produced the lowest stresses among the five investigated casing pipes. As a result, very stiff soil such as "coarse-grained soils with little or no fines" from Table 2 was assumed. For analysis of such soil, a modulus of soil reaction of 3,300 psi with 100% compaction at 5-10 feet depth of cover was utilized.

**Table 4. General Information of Collected Experimental Data**

| | Pipe OD (in) | Pipe WT (in) | DoC (in) | Installation | Soil Type | Internal Pressure (psig) |
|---|---|---|---|---|---|---|
| Battelle-AARRC | 8.625<br>24 | 0.219<br>0.25 | 27.375<br>25, 50 | Open trench | Silty sand | 0<br>0, 550 |
| Spangler | 30#<br>36#<br>42#<br>34!<br>30$ | 0.25<br>0.312<br>0.375<br>0.406<br>0.344 | 84<br><br><br>101<br>161 | Auger boring | N/A | 0 |
| Cornell-TTC | 12.75<br>36 | 0.25<br>0.606 | 69<br>69 | Auger boring | Dense sand | 0* |

\# At Thorsby, Alabama
! At Gallup, New Mexico
$ At Garden City, Iowa
* The experiments also investigated non-zero internal pressure. However, only the maximum stress under zero internal pressure was reported in reference [8] for both pipes.

**Table 5. Live Load Information in Collected Experimental Data**

| | Pipe OD (in) | Loading Method | Load Amplitude (kips) |
|---|---|---|---|
| Battelle-AARRC | 8.625 | Steel plate | 10, 15 |
| | | Three-tie track segment | 18, 36, 54, 72, 95 |
| | 24 | Concrete slab | 25 |
| | | Steel plate | 25 |
| | | Three-tie track segment | 95 |
| Spangler | 30 to 42 | Single train passing the tracks on top of pipe | N/A |
| Cornell-TTC | 12.75, 36 | Single train parking on tracks on top of pipe | N/A |

**Table 6. Input Parameters for Kiefner Approach**

| | Pipe OD (in) | E' (psi) | Bedding Angle (deg) | $F_{\text{impact}}$ |
|---|---|---|---|---|
| Battelle-AARRC | 8.625<br>24 | 1200, 1900<br>1200 | 30 | 1.0 |
| Spangler | 30<br>36<br>42<br>34<br>30 | 3300<br>2700<br>2000 | 120 | 1.5 |
| Cornell-TTC | 12.75<br>36 | 1800* | 120 | 1.0* |

* Following the value provided in reference [8]

i The pipe dimensions and buried depths have been listed in Table 4 and Table 5 and are not repeated in Table 6.
ii There is a very coarse estimation as the stresses level in the pipe also depends on the dimensions of pipes, applied loads and other factors.

 

At Garden City, Iowa, the 30-inch pipe was buried at the greatest depth of nearly 13 feet, but the highest stress was measured. Therefore, very soft soil such as “fine-grained soils with less than 25% sand content” was assumed. For analysis of such soil, a modulus of soil reaction of 2,300 psi with 100% compaction at 10-15 feet depth of cover was utilized. Finally at Gallup, New Mexico, the 34-inch pipe was buried at a moderate depth of around 8 feet with moderate measured stress. The soil type assumed was “coarse-grained soils with fines”. For analysis of such soil, a modulus of soil reaction of 2,700 psi with 100% compaction at 5-10 feet depth of cover was utilized. For Cornell-TTC experiments, a soil modulus of reaction of 1800 psi was reported in reference [8].

The bedding angle was used to determine the parameters $K_\mathrm{b}$ and $K_\mathrm{z}$ in equation (2). The bedding angle depends on the installation method of the pipe. In the Battelle-AARRC experiments, the pipes were installed through the open trench method. As a result, the bedding angle was conservatively selected as 30°. In the Spangler experiments and the Cornell-TTC experiments, the casing pipes and line pipes were installed through the auger boring method beneath the railroads. The bedding angle was therefore selected as 120°.

The impact factor, $F_\mathrm{impact}$, was determined from loading condition in the tests. In the Battelle-AARRC experiments, all the live loads were applied as static loads. As a result, the impact factor was 1.0. In the Spangler experiments, the stress was measured when moving trains passed along the tracks over the pipes. Therefore, the maximum impact factor of 1.5 was used. In Cornell-TTC experiments, an impact factor of 1.0 for the tests was reported in reference [8].

One parameter not covered in Table 6 is the spring coefficient, $k$, used in equation (9) to predict the longitudinal stresses. This parameter was determined using the soil spring model following the procedure in Annex A. The soil spring model requires the soil properties including the weight of soil per unit volume, $\gamma$, friction angle, $\phi$, and cohesion, $c$. No detailed soil properties other than soil type were recorded during the experiments. For Battelle-AARRC experiments, $\gamma$ = 120 lb/ft$^3$, $\phi$ = 30° and $c$ = 0 were used. These are typical parameters for loose sand which was close to the silty sand soil used in the experiments. For Cornell-TCC experiments, $\gamma$ = 120 lb/ft$^3$, $\phi$ = 40° and $c$ = 0 were used, which are typical parameters for dense sand at the experimental site. As no longitudinal stresses were measured in Spangler experiments, no estimation for $k$ was needed.

The live loads on the ground surface were simulated as follows. In the Battelle-AARRC experiments, three loading configurations were used. The steel plate was simulated as a single point load. The concrete slab was simulated by a grid of small rectangles covering a 6-foot by 8-foot area. The total load of 25 kips was then uniformly distributed among the grid. The three-tie track segment was simulated by a series of concentrated loads distributed along three lines. Each line was along the centerline of a tie. The total live load applied on the track was then distributed uniformly along the three lines. For the Spangler and the Cornell-TCC experiments, the live load from the real train was simulated by a grid of small rectangles with the concentrated load at the center of each rectangle. The amplitude of the concentrated load was determined by the area of the rectangle and the pressure derived from uniformly distributing the 320-kips weight of the loaded train car over an area of 20-feet by 8-feet[iii].

## Analysis with Current API RP 1102 Approach

The formulae estimating the stresses in API RP 1102 involve multiple factors. API RP 1102 provides multiple figures with curves that can used to determine the values of these factors, with input parameters such as pipe dimensions, soil properties, and pipe burial depth. The curves in these figures are only provided for pipe diameter/wall thickness ratios less than 100, and buried pipe depths greater than 6 feet for railroad crossings or greater than 3 feet for highway crossings. These specified ranges are due to the investigated range of FEA from which these curves were developed [8].

The input parameters[iv] for the analysis with the API RP 1102 approach are listed in Table 7.

API RP 1102 requires soil resilient modulus, $E_\mathrm{r}$, to predict the stresses resulting from a live load. API RP 1102 provides suggested values for $E_\mathrm{r}$ for various soil types[v]. Following the soil types discussed in the previous section of “Analysis with Kiefner Approach”, the estimated $E_\mathrm{r}$ values are listed in Table 7.

API RP 1102 also has its own recommendation for impact factor, $F_\mathrm{i}$, based on road type and buried depth[vi]. In the Battelle-AARRC experiments, all the live loads were applied as static loads. As a result, the impact factor is 1.0. In the Spangler experiments, the stress was measured when trains passed over the tracks on top of the pipes. Due to this dynamic loading, impact factors greater than 1.0 were determined following the approach in API RP 1102. In the Cornell-TTC experiments, an impact factor of 1.0 for the tests was reported in reference [8].

**Table 7. Input Parameters for API RP 1102 Approach**

| | Pipe OD (in) | $E_\mathrm{r}$ (ksi) | $F_\mathrm{i}$ |
|---|---|---|---|
| Battelle-AARRC | 8.625<br>24 | 10 | 1.0 |
| Spangler | 30<br>36<br>42 | 20 | From API RP 1102 |
| | 34 | 10 | |
| | 30 | 5 | |
| Cornell-TTC | 12.75<br>36 | 20* | 1.0* |

* Following the value provided in reference [8]

[iii] This is a typical design train load known as Cooper E-80. Please see reference [9] for details.
[iv] The pipe dimensions and buried depths have been listed in Table 4 and Table 5 and are not repeated in Table 7.
[v] Table A-2 in reference [9].
[vi] Figure 7 in reference [9].

The API RP 1102 approach uses the pressure on the ground surface, $w$, to determine the stresses resulting from a live load. There are also different formulae for stresses due to live loads depending on whether the live load is from a railroad or a highway. The selection of formulae and the values of $w$ are summarized in Table 8.

**Table 8. Load Configuration Treatment for Analysis with API RP 1102 Approach**

| | Loading Method | API RP 1102 Formulae | Pressure on the Ground, $w$ (psi) |
|---|---|---|---|
| Battelle-AARRC | Concrete slab | Highway formulae with rigid pavement and single axle | 86.8 |
| | Steel plate | Highway formulae with no pavement and single axle | 56.6 – 141.5 |
| | Three-tie track segment | Railroad formulae | 2.94 - 15.5 |
| Spangler | Single train passing over the pipe | Railroad formulae | 13.9 |
| Cornell-TTC | Single train parking over the pipe | Railroad formulae | 13.9 |

In Battelle-AARRC experiments, three loading configurations were used. The concrete slab simulated the load on a road with rigid pavement. As a result, the highway formulae were used with a pavement type factor, $R$, of 0.9 and an axle configuration factor, $L$, of 0.65 [vii]. The ground pressure, $w$ = 25,000/(2×144) = 86.8 psi, was determined by considering that the application of total 25 kips load on slab was equivalent to the application of the load of a single axle via two wheels. This value is very close to the design value of 83.3 psi for a single axle truck recommended in [9]. The steel plate simulated a single point load on an unpaved ground surface, for which the highway formulae were selected with $R$ = 1.20 and $L$ = 0.80 for the 8.625-inch pipe and $R$ = 1.10 and $L$ = 0.65 for the 24-inch pipe[viii]. The ground pressure is calculated as $w = F/\pi(d_0/2)^2$, where $F$ is the applied force and $d_0$ is the diameter of the plate (in this case 15 inches). Three loads of 10 kips, 15 kips and 25 kips were applied during the experiments, resulting in $w$ values of 56.6 psi, 84.9 psi, and 141.5 psi, respectively. The three-tie track segment simulated the railroad loads, for which the railroad formulae were selected. The ground pressure, $w$, was determined by distributing the total force uniformly over an area of 102 inches by 60 inches[ix]. For the maximum load of 95 kips applied via the three-tie track segment, the result is $w$ = 15.5 psi, which is very close to the design value of 13.9 psi for the Cooper E-80 loaded train car recommended in [9]. For the Spangler and the Cornell-TCC experiments, the live load from the real train was applied. Therefore, the railroad formulae were selected, and the design value of $w$ = 13.9 psi for the Cooper E-80 load was used.

### Results Comparison

The comparison between the measured hoop stresses from all collected experimental data and the prediction from the Kiefner approach and the API RP 1102 approach is presented in Figure 3. The blue dots show the predictions from the Kiefner approach and the red dots show those from the API RP 1102 approach. The red dots with a cross indicate the cases that are out of the range of the curves in API RP 1102 to determine the factors used to predict the stresses. For such cases, we used the stress factors determined by the available points on the curves which were closest to the experimental conditions. However, the accuracy of these dots may be arguable. From the figure, the Kiefner approach provided a consistently conservative estimation for all cases with a mean factor of around 2.5. The API RP 1102 approach predicted lower stresses than the Kiefner approach. There are many cases that were out of the range of the API RP 1102 approach. For a considerable proportion of cases, the predicted stresses from the API RP 1102 approach were also nonconservative. Even if one were to neglect the out-of-range cases, there are still several cases with predicted stresses from the API RP 1102 approach that are lower than measured values from the experiments. The comparison between the measured longitudinal stresses from all collected experimental data, the prediction from the Kiefner approach, and the API RP 1102 approach is presented in Figure 4, with trends similar to those of the hoop stresses. For longitudinal stress, the Kiefner approach provided a conservative estimation for all cases except one. However, the mean factor was around 1.3 which was lower than that for the hoop stress. The API RP 1102 approach predicted lower stresses than the Kiefner approach and the predictions were nonconservative for a considerable proportion of cases, even neglecting those which were out of the range of the API RP 1102 approach.

The API RP 1102 approach was developed based on FEA modeling for bored pipe and later was verified through experiments on bored pipes. However, the API RP 1102 approach may underestimate the stresses in pipes installed by the open trench method where the pipe receives less support from the surrounding soil (in the Kiefner approach this translates to a lower bedding angle for a pipe installed by open trench method as compared to a similar bored pipe). In the three groups of experiments, the pipes in the Battelle-AARRC experiments were installed with the open trench method and the pipes in the other two groups of experiments were installed with the auger boring method. Figure 5 shows the comparison of hoop stress predictions with Spangler and Cornell-TTC experiments only. The API RP 1102 approach only

---

[vii] Following Table 2 in reference [9] for rigid pavement with a single axle load.

[viii] Following Table 2 in reference [9] for no pavement with a single axle load.

[ix] According to the test setup, the length of each tie was 8.5 feet or 102 inches, the width of the tie was 9 inches, and the space between the closest edges of two adjacent ties was 11 inches. Therefore, each tie distribute its load in an area of 102 inches by 20 inches (=11+9). Finally, the total load was distributed by three ties to an area of 102 inches by 60 inches (=3×20).

underestimated the stress in one case[x]. The predictions were conservative for all other cases including those out of the application range. However, a closer observation showed that the predictions did not follow the same trend as the measured stresses. The four red dots at the right side of the figure showed decreased predicted stresses with increased measured stresses, even though they were within the application range of the API RP 1102 approach. The predictions from the Kiefner approach were conservative for all cases and overall followed the same trend with the measured stresses. Figure 6 shows the comparison of longitudinal stress for the Cornell-TTC experiments (no longitudinal stress was reported for the Spangler experiments). The Kiefner approach predicted a higher longitudinal stress than the API RP 1102 approach for one case and was almost identical with the API RP 1102 approach for the other case. The predictions from both approaches were conservative. The inconsistent trend between the API RP 1102 predictions and the measured hoop stress may be due to the inaccurate assumption of soil types at the sites in the Spangler experiments. However, the Kiefner approach provided the same trend as the experimental results using the same assumed soil types.

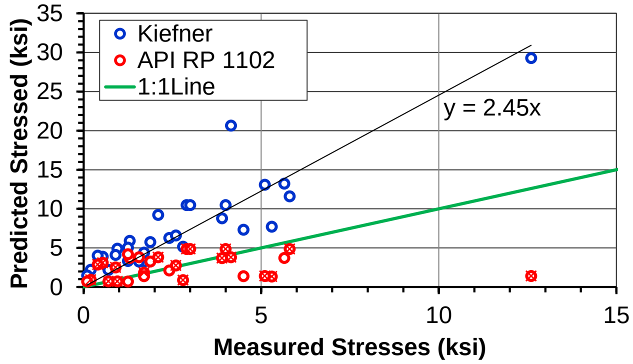


**Figure 3. Comparison of Hoop Stress with All Collected Experimental Data**

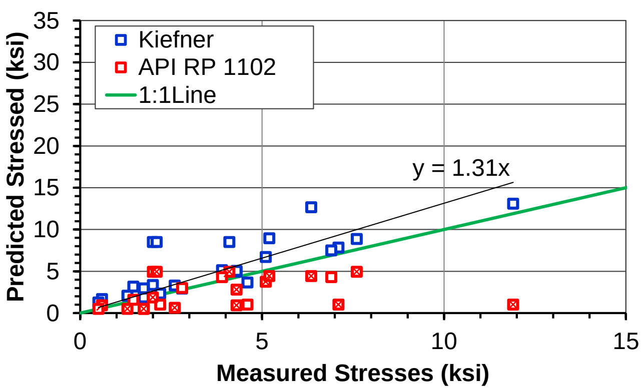


**Figure 4. Comparison of Longitudinal Stress with All Collected Experimental Data**

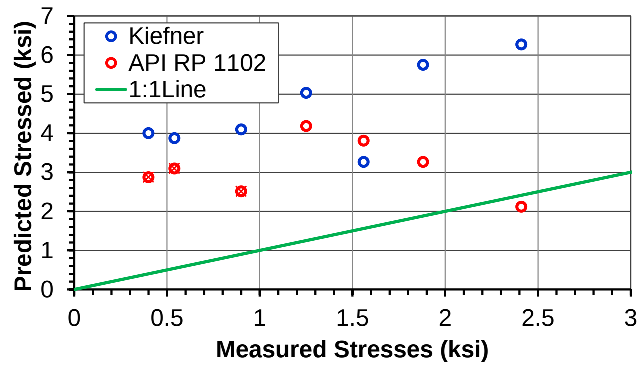


**Figure 5. Comparison of Hoop Stress with Experimental Data from Spangler and Cornell-TTC**

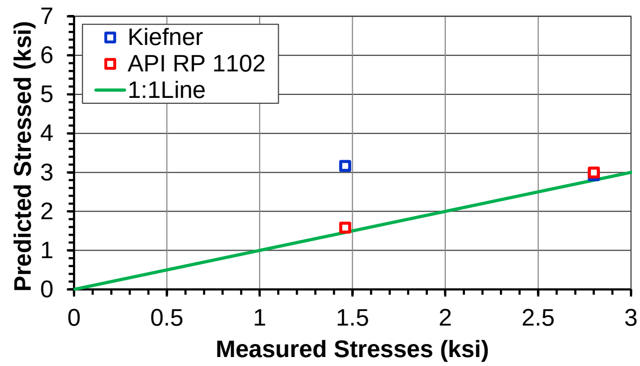


**Figure 6. Comparison of Longitudinal Stress with Experimental Data from Cornell-TTC**

The comparison with the Battelle experiments was further investigated in Figure 7 and Figure 8 for hoop stress and longitudinal stress, respectively. The steel plate and concrete slab simulated the road crossing and the three-tie track segment simulated the railroad crossing. The Kiefner approach did not distinguish the road crossing and railroad crossing. The only differences between the two types of crossing in the Kiefner approach were the live load distribution and the impact factor. The API RP 1102 approach used different groups of equations for the road crossing and railroad crossing. From Figure 7 and Figure 8, the Kiefner approach only slightly underestimated the longitudinal stress at a single case. The API RP 1102 approach underestimated the stresses for both the road crossing and railroad crossing when the pipe was installed using the open trench method. The 8.625-inch pipe with 27.375-inch DoC and the 24-inch pipe with 25-inch DoC exceeded the application range of API RP 1102. However, both conservative and nonconservative predictions were observed on the two pipes. The 24-inch pipe with 50-inch DoC was within the application range of API RP 1102. The nonconservative stresses were predicted for concrete loads and three-tie track loads on this pipe with zero internal pressure and for steel plate loads on this pipe with both zero internal pressure and 550 psig

[x] This case was Cornell-TTC experiment on 36-inch pipe. In Table 9 of reference [8], the reported measured hoop stress and predicted hoop stress were 2410 psi and 2030 psi, respectively.

internal pressure. A brief summary of the observation is that the API RP 1102 approach is not conservative for pipes installed with open trench method.

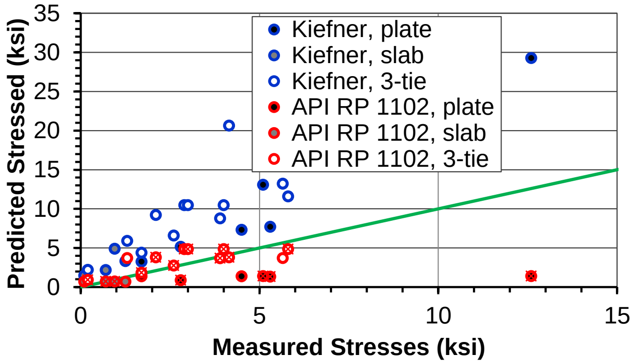


**Figure 7. Comparison of Hoop Stress with Experimental Data from Battelle-AARRC**

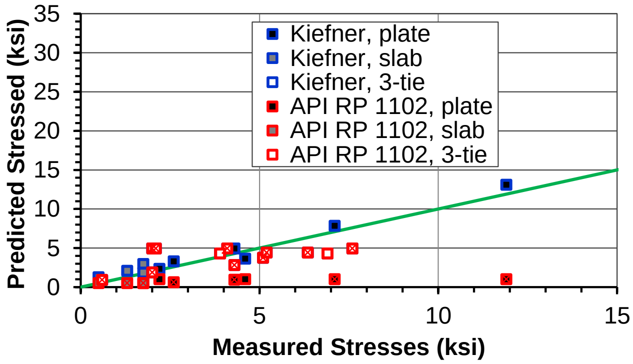


**Figure 8. Comparison of Longitudinal Stress with Experimental Data from Battelle-AARRC**

## DISCUSSION

Based on the comparison with the experimental data in the above section, the Kiefner approach provided conservative estimates in most scenarios, and in more scenarios than the API RP 1102 approach. Furthermore, the overall trends of the predictions were consistent with the observations in the experiments. The API RP 1102 approach underestimated the stresses for multiple cases when compared with the experiments, and the trends were not always consistent with the experimental observation.

The Kiefner approach is a more universal tool to treat a wide range of parameters on buried pipes under surface loading. It is applicable to problems with a wide range of pipe dimensions, buried conditions, loading scenarios, and pipe installation methods. On the contrast, the approach in API RP 1102 was developed based on pipe that was installed through boring with a relatively narrowed range for input parameters.

Under some conditions, the prediction from the Kiefner approach may be too conservative, especially for hoop stress. This stems from the usage of the Boussinesq equation. The Boussinesq equation assumes homogeneous elastic soil. In reality, the ground above buried pipes generally consists of multiple layers with quite different properties. Soil also yields under large live loads and deviates significantly from the behavior of elastic material. However, due to the complexity of the surface loading problem on buried pipes, a relatively large safety margin seems unavoidable to ensure the predictions are always conservative.

The degree of conservatism in the Kiefner approach is different for hoop stress and longitudinal stress. By comparison with the experiments data used in this study, the Kiefner approach overestimated the hoop stress by an average factor of 2.5 and overestimated the longitudinal stress by an average factor of 1.3. The longitudinal stress resulting from live load has two contributions: one from local bending which is dependent on the hoop stress due to live load, and the other from global bending which is independent of the hoop stress. The level of overestimation for the global bending component may be one of the sources that results in a different estimation level between hoop stress and longitudinal stress. However, the deviation between the predicted levels still seems a little too large. Further work may improve the model.

Finally, the approach in this paper only estimates the stresses resulting from surface loading. These stresses should be added to other existing stresses[xi] in the pipes to determine the total stresses for design or integrity assessment purpose.

## CONCLUSION

Kiefner's approach to estimate the stress in buried pipes under surface loading is presented in this paper. This approach considers both hoop stress and longitudinal stress resulting from surface loading. The stiffness effect of internal pressure and the support of soil at the sides of the pipe are also accounted for in this approach. The approach is a universal tool that is able to handle a wide range of loading scenarios.

The comparison with experimental results shows that the Kiefner approach provides a conservative estimate and overall consistent trend with the results observed. The comparison of these results with predictions from the API RP 1102 approach also showed superior performance of the Kiefner approach.


## ACKNOWLEDGMENTS

The authors would like to express their appreciation to Mr. Robert Francini for his pioneering work before retiring from Kiefner, which is the foundation of the approach introduced in the paper. The authors would also like to thank Mr. Michael Rosenfeld and Dr. John Kiefner for providing references on experimental data and for reviewing the paper.


[xi] These stress including operational stresses generated by internal pressure and temperature variation in the pipe, as well as stresses generated by external loads other than surface loads.

 

## REFERENCES


1. Spangler, M.G., “The Structural Design of Flexible Pipe Culverts”, Bulletin 153, Iowa Engineering Experiment Station, Ames, Iowa, 1941.
2. Spangler, M.G., and Hennessy, R.L., “A Method of Computing Live Loads Transmitted to Underground Conduits”, Proceedings Highway Research Board, 26:179, 1946.
3. Spangler, M.G., “Secondary Stresses in Buried High Pressure Pipe Lines”, The Petroleum Engineer, November, 1954.
4. Spangler, M.G., “Pipeline Crossing under Railroads and Highways”, Journal of the American Waterworks Association, August, 1964.
5. API Recommended Practice 1102, 5th Ed., “Recommended Practice for Liquid Petroleum Pipelines Crossing Railroads and Highways”, November 1981.
6 Stewart, H.E., and O’Rourke, T.D., “Live Loads for Pipeline Design at Railroads and Highways”, Pipeline Crossings: Proc. of a Specialty Conference Sponsored by the Committee on Pipeline Crossings of the Pipeline Division of the American, Denver, CO, March 1991.
7. Ingraffea, A.R., O’Rourke, T.D., and Stewart, H.E., “Technical Summary and Database for Guidelines for Pipelines Crossing Railroads and Highways”, Cornell University School of Civil and Environmental Engineering Final Report to Gas Research Institute, GRI-91/0285, Dec. 1991.
8. Stewart, H.E., Ingraffea, A.R., O’Rourke, T.D., and Behn, M.T., “Design of Uncased Pipelines at Railroad and Highway Crossings”, American Petroleum Institute Distribution/Transmission Conference, Houston, TX, April 7-8, 1992.
9. API RP 1102, 6th Ed., “Steel Pipelines Crossing Railroads and Highways”, 6th Ed., April 1993 (reaffirmed July 2002).
10. Warman D.J., Chorney, J., Reed, M., and Hart, J.D., “Development of a Pipeline Surface Loading Screening Process”, IPC2006-10464, Proc. of 6th International Pipeline Conference, Calgary, Canada, September 25-29, 2006,
11. Warman D.J., Hart, J.D., and Francini, R.B., “Development of a Pipeline Surface Loading Screening Process & Assessment of Surface Load Dispersing Methods”, Kiefner Report to Canadian Energy Pipeline Association, 2009.
12. Francini, R.B., and Gertler, R.C., “Field Validation of Surface Loading Stress Calculations for Buried Pipelines”, PR-218-104509, Milestone 1 Report for Pipeline Research Council International, July, 2014.
13 Van Auker, M., and Francini, R.B., “Canadian Energy Pipeline Association (CEPA) Surface Loading Calculator User Manual”, Kiefner final report 14-017, downloadable from www.kiefner.com.
14. American Lifelines Alliance, “Guidelines for the Design of Buried Steel Pipe”, July 2001 (with addenda through February 2005).
15. Pierce, R.N., Lucas, O., Rogers, P., and Rankin, C.L., “Design Procedure for Uncased Natural-Gas Pipeline Crossings of Roads and Highways”, Transportation Research Record, 1977, 631: 52-56.
16. Hartley, J.D. and Duncan, J.M., “E’ and its Variation with Depth”, ASCE Journal of Transportation Engineering, 113(5), 1987.
17. Young, W.C., Roark’s Formulas for Stress & Strain, 6th Ed., 1989, McGraw Hill.
18. Boresi, A.P., and Schmidt, R.J., Advanced Mechanics of Materials, 6th Ed., 2003, John Wiley & Sons, Inc. Chapter 10.
19. Moser, A.P., Buried Pipe Design, Second Edition, 2001, McGraw Hill.
20. Rodabaugh, E.C., Atterbury, T.J., and Hinueber, G.L., “Summary Report on Experimental Evaluation of Simulated Uncased Pipeline Crossings of Railroads and Highways”, Battelle Summary Report for Research Council on Pipeline Crossings of Railroads and Highways of American Society of Civil Engineers, July 1971.
21. Spangler, M.G., “Experimental Study of the Structural Performance of Pipeline Casing Pipes under Railroads and Highways”, Journal of the Pipeline Division, ASCE, Vol 91, No. PL1, Proc. Paper 4419, July, 1965.


## ANNEX A

### DETERMINE THE COEFFICIENT OF FROM PIPE SOIL INTERACTION MODEL

The spring coefficient of soil resisting pipe deflection, $k$, used in equation (9) can be determined by soil properties via the pipe soil interaction model. A soil spring model [14] was developed to describe the interaction force between the soil and the pipe. In the soil spring model, the maximum soil force resisting the downward deflection of a buried pipe with a unit length is known as the bearing soil force, $Q_d$, which is determined as

$$Q_{\mathrm{d}} = N_{\mathrm{c}} c D + N_{\mathrm{q}} \bar{\gamma} \left( H + \frac{D}{2} \right) D + N_{\gamma} \gamma \frac{D^2}{2} \tag{A-1}$$

where $N_{\mathrm{c}}$, $N_{\mathrm{q}}$, $N_{\gamma}$ are bearing capacity factors, $c$ is the soil cohesion, $D$ is the pipe outside diameter, $\gamma$ is the weight of the soil per unit volume, $\bar{\gamma}$ is the effective weight of soil, which equals $\gamma$ for pipe buried above the ground water level, and $H$ is the depth of cover.

The bearing capacity factors are determined by the friction angle of the soil, $\phi$, in degrees, as

$$N_{\mathrm{c}} = \cot \tilde{\phi} \left[ e^{\pi \cdot \tan \tilde{\phi}} \tan^2 \left( 45 + \frac{\tilde{\phi}}{2} \right) - 1 \right] \tag{A-2}$$

 

$$N_{\mathrm{q}} = e^{\pi \cdot \tan\phi} \tan^2\left(45 + \frac{\phi}{2}\right) \quad \text{(A-3)}$$

and

$$N_{\gamma} = e^{(0.18\phi - 2.5)} \quad \text{(A-4)}$$

In equation (A-2), $\tilde{\phi} = \phi + 0.001$. When the amplitude of soil force just reaches $Q_{\mathrm{d}}$, the critical relative displacement between soil and buried pipe is $\Delta_{\mathrm{qd}}$. For granular soils,

$$\Delta_{\mathrm{qd}} = 0.1D \quad \text{(A-5)}$$

and for cohesive soils,

$$\Delta_{\mathrm{qd}} = 0.2D \quad \text{(A-6)}$$

Finally, the spring coefficient is determined as

$$k = \frac{Q_{\mathrm{d}}}{\Delta_{\mathrm{qd}}} \quad \text{(A-7)}$$